JOURNAL OF CHEMICAL & ENGINEERING DATA

ARTICLE

pubs.acs.org/jced

Rescaled Specific Volume Model for Electrolyte Solution Density

Stephen F. Agnew*

Columbia Energy and Environmental Services, Inc., 1806 Terminal Drive, Richland, Washington 99354, United States

ABSTRACT: A very useful model, the Laliberte—Cooper (LC) model, for predicting densities for electrolyte mixtures has been previously reported that scales with mass fraction or molal electrolyte concentrations (Laliberte, M.; Cooper, W. E. Model for Calculating the Density of Aqueous Electrolyte Solutions. *J. Chem. Eng. Data* **2004**, *49*, 1141—51). This model proves to be very useful in predicting densities of even very complex mixtures such as high level waste liquids at the Hanford Site. Moreover, a straightforward rescaling of the LC model results in a much more intuitive basis. As a result, this rescaled LC (RLC) model reveals much insight into the free energy changes associated with electrolyte specific volumes. Moreover the introduction of an additional parameter for total cation scaling extends the RLC to molar concentrations.

INTRODUCTION

Previous work has shown[1] that the density of complex electrolyte solutions can be calculated based on a set of empirical parameters and the known mass fractions of each species. This model, termed the LC (Laliberte—Cooper) model, was recently extended to aluminate solutions[2] and accurately describes pure electrolyte solution densities over large ranges of concentrations and temperatures.

Once reconstituted for treatment, there will be hundreds of millions of gallons of complex mixtures of electrolytes from waste tanks at both Hanford and Savannah River Sites, and predicting density based on composition is important for processing these liquids. To further enhance the LC model and better apply it to complex mixtures, this paper shows how a straightforward rescaling of the LC parameters results in a much more intuitive basis. That is, although the LC model expresses apparent molar volume changes as a function of molal concentration very well, the physical bases for these scaled parameters are not very clear.

Accurate density predictions for arbitrarily complex electrolyte mixtures has been a challenge for nuclear waste mixtures. Typically, models used for nuclear waste scale on relatively coarse parametrizations of total ionic strength or total sodium and application of the LC model have substantially improved predictions[2] over previous models.

Rescaling the LC temperature dependence into a product of linear and Arrhenius temperature parameters further improves the rescaled LC (RLC) physical basis. This RLC model represents each apparent volume as a molal scaling between two limiting specific volumes with each of those two limiting volumes scaled with temperature factors as well. However, it is important to recognize that the RLC parameters are not adjusted in any way to fit new data. Rather, the RLC and therefore the LC parameters are simply being applied to a large existing data set.

It is very desirable to also have a variation of the density model based on electrolyte mass per total volume (i.e., molar units). Given one additional parameter, a limiting cation concentration, this paper also describes a variation that is dependent on volume scaling (molar units) instead of mass fraction scaling (i.e., molal units). This single parameter must be fit to an existing data set.

APPROACH

The LC model represents density as a mass-weighted average of specific volumes for a mixture of electrolytes as

$$\rho = \frac{1}{f_{\text{water}}\nu_{\text{water}} + \sum f_i \bar{\nu}_{\text{app},i}} \tag{1}$$

where f_i represents the mass fraction of species i and $\nu_{\text{app},i}$ is the apparent specific volume of electrolyte i. Each electrolyte's specific volume is a parametrized equation fit to a set of four parameters as

$$\bar{\nu}_{\text{app},i} = \frac{(1 - f_{\text{water}}) + c_2 + c_3 T}{(c_0(1 - f_{\text{water}}) + c_1)e^{(0.000001(T + c_4)^2)}} \tag{2}$$

and these parameters are adjusted for a least-squares fit over some data set. The LC expression has proven very useful, and a straightforward rescaling of its parameters increases its physical basis and intuitive appeal. Furthermore, reformulating the temperature dependence as a product of linear expansion and Arrhenius factors further shows the scalability of this powerful model.

A variation of the LC model that is appropriate for molar concentration scaling instead of molal scaling is also developed. In both cases, the density model is only applicable to electrolyte solutions.

Rescaled LC (RLC) Specific Volume (Molal) Density Model. Rewriting eq 2 in terms of three new parameters ν_{0i}, ν_{1i}, and f_{water} (f_{water}, water weight fraction) results in

$$\bar{\nu}_{\text{app},i} = \frac{(1 - f_{\text{water}})k_i + \nu_{0i}}{(1 - f_{\text{water}})((k_i + \nu_{0i})/\nu_{1i} - 1) + 1} \tag{3}$$

which is functionally equivalent but provides much more insight into the nature of the LC model, now termed the RLC model. The apparent specific volume for electrolyte i, ν_i, scales between two limits, ν_{0i} and ν_{1i}, which represent the limiting specific volumes for each electrolyte in infinite dilution, ν_{0i} ($f_i \rightarrow 0$), versus

Received: July 20, 2011
Accepted: October 31, 2011
Published: November 29, 2011

a hypothetical specific volume, v_{1i} ($f_i \rightarrow 1$), of each "dry" electrolyte with the scaling between these two limits set by k_i. That is, with increasing k_i, there is more curvature in the trend of $v_{\mathrm{app},i}$ versus mass fraction.

The RLC density equation is now

$$\rho = \frac{1}{f_{\mathrm{water}} v_{\mathrm{water}} + \sum f_i v_i} = \frac{1}{f_{\mathrm{water}} v_{\mathrm{water}} + \sum f_i \frac{((1 - f_{\mathrm{water}}) + v_{0i}/k_i) e^{-\alpha(T)}}{(1 - f_{\mathrm{water}})((1 + v_{0i}/k_i)/v_{1i} - 1/k_i) + 1/k_i}} \quad (4)$$

where the new parameters in terms of the original LC parameters c_0, c_1, c_2, c_3, and c_4 are

$$v_{0i} = 1000 \frac{c_{2i} + c_{3i} T}{c_{1i}} e^{-(T + c_{4i})^2/1e6} \quad (5)$$

$$v_{1i} = \frac{1000(c_{2i} + 1 + c_{3i} T)}{(c_{1i} + c_{0i})} e^{-(T + c_{4i})^2/1e6} \quad (6)$$

$$k_i = \frac{1000}{c_{1i}} e^{-(T + c_{4i})^2/1e6} \quad (7)$$

given a convenient scaling to $\mathrm{cm}^3 \cdot \mathrm{g}^{-1}$. The temperature dependences among these parameters are much more apparent, and further reducing these parameters into temperature independent and dependent factors results in

$$v_{0i}(T) = \frac{1000(c_{2i} + 25c_{3i} + (T - 25)c_{3i})}{c_{1i} e^{(25 + c_{4i})^2/1e6} e^{(T - 25)^2/1e6} e^{2(T - 25)(c_{4i} + 25)/1e6}} = v_{0i}^{25} + d_0(T - 25) \quad (8)$$

$$\alpha(T) = (T - 25)^2/1e6 + 2(T - 25)(c_{4i} + 25)/1e6 \quad (9)$$

with the reference temperature state now set to T = 25 °C as

$$v_{0i}^{25} = 1000 \frac{c_{2i} + 25c_{3i}}{c_{1i}} e^{-(25 + c_{4i})^2/1e6} \quad (10)$$

and the linear temperature factor as

$$d_0 = 1000 \frac{c_{3i}}{c_{1i}} e^{-(25 + c_{4i})^2/1e6} \quad (11)$$

Likewise the expression

$$v_{1i}(T) = \frac{1000(c_{2i} + 25c_{3i} + 1 + (T - 25)c_{3i})}{(c_{0i} + c_{1i}) e^{(25 + c_{4i})^2/1e6} e^{(T - 25)^2/1e6} e^{2(T - 25)(c_{4i} + 25)/1e6}} = v_{1i}^{25} + d_1(T - 25) \quad (12)$$

has a reference temperature state as

$$v_{1i}^{25} = \frac{1000(c_{2i} + 25c_{3i} + 1)}{(c_{0i} + c_{1i})} e^{-(25 + c_{4i})^2/1e6} \quad (13)$$

and a linear temperature factor as

$$d_1 = 1000 \frac{c_{3i}}{(c_{0i} + c_{1i})} e^{-(25 + c_{4i})^2/1e6} \quad (14)$$

The parameter k_i is

$$k_i = \frac{1000}{c_{1i} e^{(25 + c_{4i})^2/1e6} e^{(T - 25)^2/1e6} e^{2(T - 25)(c_{4i} + 25)/1e6}} = k_i^{25} \quad (15)$$

with

$$k_i^{25} = \frac{1000}{c_{1i}} e^{-(25 + c_{4i})^2/1e6} \quad (16)$$

and has no linear temperature factor.

All three RLC model parameters have the same reduced exponential temperature factor eq 9 that depends only on LC parameter c_4. Furthermore, the linear temperature factor only occurs for the two specific volume limits. The density expression is now

$$\rho = 1/\left[f_{\mathrm{water}} v_{\mathrm{water}} + \sum f_i [((1 - f_{\mathrm{water}}) + (v_{0i}^{25} + d_0(T - 25))/k_i^{25}) e^{-(T - 25)^2/1e6} e^{-2(T - 25)(c_{4i} + 25)/1e6}] / [(1 - f_{\mathrm{water}})((1 + (v_{0i}^{25} + d_0(T - 25))/k_i^{25}) / (v_{1i}^{25} + d_1(T - 25)) - 1/k_i^{25}) + 1/k_i^{25}] \right] \quad (17)$$

and the density at 25 °C reduces to simply

$$\rho = \frac{1}{f_{\mathrm{water}} v_{\mathrm{water}} + \sum f_i \frac{((1 - f_{\mathrm{water}}) k_i^{25} + v_{0i}^{25})}{(1 - f_{\mathrm{water}})[(k_i^{25} + v_{0i}^{25})/v_{1i}^{25} - 1] + 1}} \quad (18)$$

RLC Known Volume (Molar) Scaling. Given known electrolyte amounts added to a total solution volume (i.e., molar) instead of to a determined mass fraction of water (i.e., molal), it is possible to adapt a modified form of both LC and RLC variants that nevertheless scale electrolyte specific volumes and produce accurate density predictions. This provides convenient forms of the LC and RLC models for electrolyte solutions with known volumes and molar concentration units. For the molar case, the density equation is

$$\rho = \frac{\sum m_i}{V} + \rho_{\mathrm{water}} \left(1 - \frac{\sum m_i v_i}{V} \right) \quad (19)$$

where m_i is the mass of each electrolyte in grams, V is the total solution volume in cm^3, and v_i is the same apparent specific volume for each electrolyte. In the case of mixtures of sodium salts of known volume, each apparent specific volume scales between the same two limits, but now by means of a cation volume concentration fraction as

$$f_{\mathrm{cation}} = \frac{[\mathrm{Na}]}{[\mathrm{Na}]_c} \quad (20)$$

For this fractional cation scaling, eq 2 becomes for the standard LC or known-water variant

$$\bar{v}_{\mathrm{app},i} = \frac{f_{\mathrm{cation}} + c_2 + c_3 T}{(c_0 f_{\mathrm{cation}} + c_1) e^{(0.000001(T + c_4)^2)}} \quad (21)$$

dx.doi.org/10.1021/je200767f | J. Chem. Eng. Data 2012, 57, 60–65

Table 1. Rescaled Electrolyte RLC Parameters from the LC Model[a]

	v_{0i}^{25}	v_{1i}^{25}	solid specific volume	k_i^{25}				ΔS_i, entropy change
electrolyte	$cm^3 \cdot g^{-1}$	$cm^3 \cdot g^{-1}$	$cm^3 \cdot g^{-1}$	$cm^3 \cdot g^{-1}$	d_0 (x1e6)	d_1 (x1e6)	c_4 (1/T)	$J \cdot mol^{-1} \cdot deg^{-1}$
$NaAl(OH)_4$	0.32340	0.46779	0.426	0.57867	1938.5	1005.3	1502.1	8.83
$Na_2C_2O_4$	0.18278	0.58520	0.441	0.43646	1986.8	1877.5	1508.4	8.86
NaCl	0.30412	0.56173	0.462	0.22003	3217.6	3448.4	3315.6	17.8
Na_2CO_3	−0.031883	0.42421	0.395	0.83668	1785.5	941.13	3342.4	18.0
NaF	−0.095712	0.18373	0.360	2.6562	579.06	41.552	4586.9	24.1
$NaNO_2$	0.33366	0.52383	0.461	0.32793	721.44	571.23	1500	8.82
$NaNO_3$	0.34060	0.45576	0.443	0.35189	2655.0	1747.4	1819.2	10.4
NaOH	−0.08845	0.57743	0.469	0.96135	668.13	441.98	542.88	4.08
Na_3PO_4	−0.092998	0.32113	0.394	0.62677	85.868	51.650	173.71	2.25
Na_2SO_4	0.11504	0.63521	0.375	0.34348	2490.6	3450.3	4731.5	24.8

[a] All parameters are calculated directly from the LC model[1] with the equations shown in the text.

or alternatively eq 3 becomes for the known volume RLC variant

$$v_i = \frac{(f_{\text{cation}} k_i + v_{0i}) e^{-\alpha(T)}}{f_{\text{cation}}((k_i + v_{0i})/v_{1i} - 1) + 1} \tag{22}$$

Upon substitution into eq 19 the expression for density at known volume becomes

$$\rho = \frac{\sum m_i}{V} + \rho_{\text{water}} \left(1000 - \frac{\sum m_i \left(\frac{([\text{Na}] k_i + v_{0i}[\text{Na}]_c) e^{-\alpha(T)}}{[\text{Na}]((k_i + v_{0i})/v_{1i} - 1) + [\text{Na}]_c} \right)}{V} \right) \tag{23}$$

where now there is a new parameter, $[\text{Na}]_c$, which is the limiting sodium concentration of these mixtures. Normally this would be adjusted to best fit a given data set.

Arrhenius Temperature Dependence. The LC exponential temperature factor

$$e^{-\alpha(T)} = e^{-(T-25)^2/1e6} e^{-(T-25)2c_{4i}/1e6} \tag{24}$$

fits the observed density temperature dependences very well, but it is desirable for a temperature dependence scaling on a free energy change between the two volume states for each electrolyte. This would have the form of equilibrium as

$$n_{1i}/n_{0i} = e^{-\Delta g/RT} \tag{25}$$

where Δg represents a partial free energy change between these two solution volume states. Further assuming that these volume states represent a loss of one mol H_2O from "frozen" outer solvation sphere to the bulk "liquid" fixes the enthalpy differential change to a common heat of outer solvation, $\Delta H_{\text{outer}} = 399\ J \cdot mol^{-1}$. This common heat of outer solvation is simply the binding energy of water to other waters that are themselves bound to the inner solvation sphere.

$$\Delta g_i = \Delta H_{\text{outer}} - T\Delta S_i \tag{26}$$

$$e^{-\alpha(T)} = e^{-\Delta g/RT} \tag{27}$$

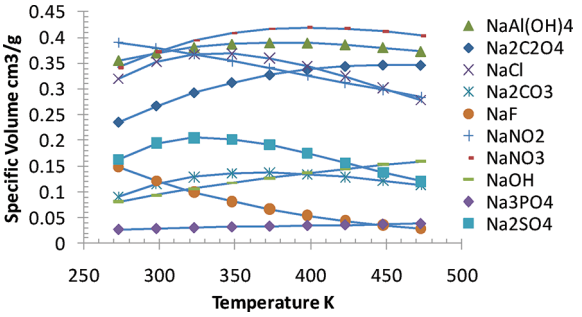

Figure 1. Plot showing specific volumes for each electrolyte at $f_i = 0.2$, eq 22. Symbols show LC calculation as eq 22 while straight lines are Arrhenius RLC calculation eq 27 fit by regression to those points.

Simply replacing the LC exponential factor with this Arrhenius factor results in

$$\rho = \frac{1}{f_{\text{water}} v_{\text{water}} + \sum f_i \frac{((1 - f_{\text{water}}) k_i + v_{0i}) e^{-\Delta g/R(1/T - 1/298)}}{(1 - f_{\text{water}})((k_i + v_{0i})/v_{1i} - 1) + 1}} \tag{28}$$

Since the enthalpy change, ΔH_{outer}, is the same among electrolytes, the Arrhenius factor represents a series of entropy changes (ΔS_i) between electrolyte volume states as listed in Table 1. The entropies and outer solvation enthalpy result from least-squares fits of the LC temperature factors as shown in Figure 1. These entropy changes result from a least-squares minimization of the differences in apparent volume between this variant which depends on LC parameter c_4. Presumably these entropies describe changes associated with each pair of electrolyte volume states. Note that this enthalpy and entropy are only some limited fractions of the total free energy of solvation.

Figure 1 shows the specific volume for each electrolyte as a function of temperature for the LC exponential factor eq 22 as data points. Each set is fit with an Arrhenius temperature exponential, eq 27, shown as lines. In each case, the sum of squares of the residual was minimized by adjusting only the entropy ΔS_i, fixing the enthalpy to that of enthalpy noted above.

dx.doi.org/10.1021/je200767f | J. Chem. Eng. Data 2012, 57, 60–65

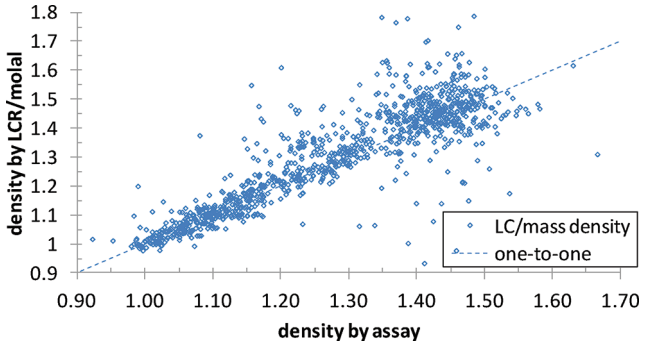

Figure 2. Scatterplot of calculated RLC density from eq 18 with electrolyte mass fractions versus measured density for ~1200 waste liquid assays. No parameters were adjusted in this calculation which showed a 2.5 % RSD (relative standard deviation) at 1.0 and a 6.6 % RSD at 1.50 g·cm^{-3}.

Table 2. Typical Compositions for Liquids at Different Densities

species	ρ = 1.21 g·cm^{-3}	ρ = 1.47 g·cm^{-3}
Na^+	5.5 M	10.9 M
OH^-	0.88 M	5.7 M
NO_3^-	2.1 M	2.9 M
NO_2^-	1.1 M	2.5 M
$Al(OH)_4^-$	0.57 M	1.2 M
CO_3^{2-}	0.18 M	0.14 M
K^+	0.04 M	0.91 M
other	~0.2 M	~0.4 M

RESULTS

This RLC model is simply a restatement of the LC model parameters, and so the RLC calibration is fundamentally just the LC calibration restated.

Table 1 compares the limiting specific volumes for each electrolyte with the specific volume for each corresponding solid. In nearly all of these examples, the v_{1i} exceeds each solid's specific volume with exceptions for NaF and Na_3PO_4. Especially for NaF, there is a factor of two smaller specific volumes which suggests a very strong electrostriction for this electrolyte in solution that persists to high ionic strength. Of course, electrostrictive polarization of water molecules by aqueous ions is a well-known phenomenon[3−5] and readily explains the v_{0i}'s decreased volume for each of the electrolytes.

The linear temperature terms for each of v_{0i} and v_{1i} have parameters d_0 and d_1, respectively, and Table 1 shows these parameters.

Figure 2 shows the scatter plot for a set of ~1200 assays of Hanford waste tank liquid densities[6] versus the calculation of eq 18. This RLC form is the mass fraction or molal basis, and there does appear to be both a scatter and bias in this model relative to the data. Table 2 lists typical liquid compositions for dominant electrolytes at two different densities.

Figure 3 shows the scatter plot for the same set of ~1600 assays of Hanford waste tank liquids[6] versus the molar RLC calculation of eq 23. The parameter $[Na]_c$ = 16.0 was the result of constraining the slope of the scatter plot regression to 1.0003. The result shows a somewhat reduced bias with a similar scatter as with the mass fraction RLC fit.

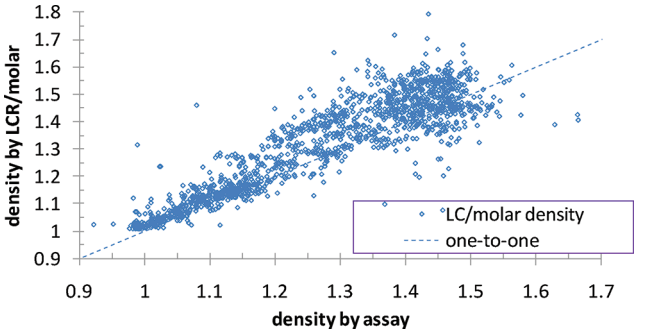

Figure 3. Scatterplot of calculated density for molar RLC (eq 23) versus measured density for ~1600 waste liquid assays given $[Na]_c$ = 16.0 M with 3.5 % at 1.0 and 6.0 % at 1.5, adjusted for best fit by minimizing RSD.

DISCUSSION

With increasing concentration, the variability of the RLC/molal density predictions increases over that expected from assay error, from 2.5 % to 6.6 % RSD (relative standard deviation) from ρ = 1.0 to 1.5 g·cm^{-3} with an *R*-square of 0.995 for the whole data set. This 2.5 increase in scatterplot variability for RLC/molal (and indeed LC) density predictions as solution concentration increases suggests that these complex electrolyte mixtures do not behave in a systematic manner.

These liquid compositions are dominated by certain ions at different concentrations as listed in Table 2, but the LC model calibration works well even at high concentrations for simple mixtures.[1,2] So the reason that increasing concentration apparently leads to both increases and decreases in pure electrolyte specific volumes for these mixtures is not yet clear.

There was a systematic bias in measured versus calculated water contents for this data set of about (2 to 7) % less measured than calculated. Therefore the calculated water contents were used for the RLC/molal prediction. Water content is not a factor with the RLC/molar prediction.

The rescaled LC specific volume model is a variation of the LC model that reveals more about its underlying physical basis and therefore affords a more intuitive interpretation for its parameters. The RLC model parameters have ready interpretations making certain correlations among the parameters very compelling.

For example, the parameter k_i, which describes the curvature of $v_{app,i}$ versus f_i, appears to reflect the strength of electrostriction as shown in Figure 4. This is because k_i is greatest for those electrolytes associated with negative v_{0i} and therefore large electrostrictions: NaF, NaOH, Na_2CO_3, and Na_3PO_4. Correspondingly, this parameter appears smallest for NaCl electrolyte, which has a positive v_{0i}, and other simple electrolytes, $NaNO_3$, $NaNO_2$, and $NaAl(OH)_4$.

Table 1 shows that the linear thermal parameters, d_0 and d_1, are very similar for the two different limiting specific volumes, v_{0i} and v_{1i}. It is very likely for first order that $d_0 = d_1$, and the fact that they are different is simply related to the manner of the original LC model parametrization. These parameters are related to volumetric thermal expansion coefficients as $d_0 e^{\Delta S/R}$ and $d_1 e^{\Delta S/R}$, which are 464e-6 and 497e-6, respectively, for NaCl from Table 1.

A reported[7] thermal expansion coefficient of 25 wt % brine at 25 °C is 398e-6, while that of water[8] is 207e-6 at 20 °C. Thus,

dx.doi.org/10.1021/je200767f |*J. Chem. Eng. Data* 2012, 57, 60–65

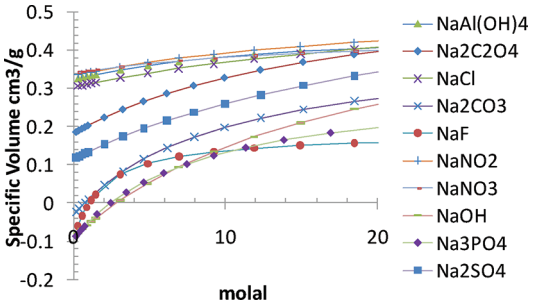

Figure 4. Plots of specific volume versus molality for electrolytes as shown. Each electrolyte specific volume ranges between two limits, v_{0i} and v_{1i}, as a function of mass fraction or molality. The rate of change between the limits set by k_i.

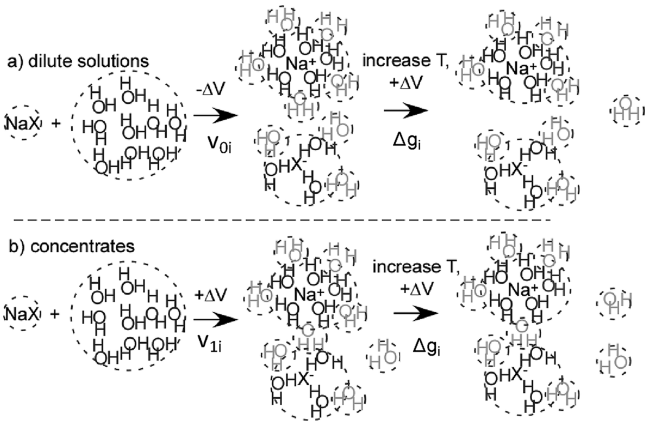

Figure 5. Depictions of dilute and concentrated solvation volume states for an electrolyte, NaX. The dilute solution volume state (a) has decreased volume relative to its solid due to solvent electrostriction, strongly bound water (dark) plus weakly bound water (light). The concentrated volume state (b) shows increased volume relative to the dilute state due to displacement of an outer water as shown. Each volume state also shows increased volume with temperature as a result of both thermal expansion and one less water from a "frozen" outer-shell water.

thermal expansion coefficients associated with the linear temperature factors seem to be consistent with previous reports for brines.

The structure of the original LC model showed an exponential temperature factor in eq 2 common to all electrolytes, $\exp(-0.000001T^2)$, but it was not very clear why that was so. The RLC model temperature dependence now includes an Arrhenius form in the RLC model, and it is now clear that the constant factor was related to common enthalpy of outer hydration as $\exp(-399\ \mathrm{J\cdot mol^{-1}}/RT)$ in eq 23.

Despite the very intuitive nature of many of these parameters, a complete microscopic model is still somewhat lacking. A common enthalpy change among these varied electrolytes suggests that each electrolyte has two solvation states that differ by one equivalent of outer sphere water. This particular outer water is weakly bound to other inner coordinated waters and not strongly bound to an ion meaning that this outer water represents an outer sphere hydration. An increase in temperature in effect "melts" that one water from an ion's outer solvation resulting in a transition between specific volumes for that electrolyte.

Since all of the electrolyte ΔS_i are positive, the higher temperature solvent clusters have increased their number of states similar to the entropy increase that occurs for melting a mole of water at 25 °C, +22 $\mathrm{J\cdot mol^{-1}\cdot K^{-1}}$. Note that the enthalpy change for outer hydration, 399 $\mathrm{J\cdot mol^{-1}}$, is only about 7 % of that of melting ice, 6.0 $\mathrm{kJ\cdot mol^{-1}}$. Recent calculations seem to be consistent with this result and show[9] that the outer water dipole moment for K^+ and Ca^{2+} ions is about 7 % less than that of bulk water, 0.2 D versus 3.0 D.

Dispersive interactions among water molecules are very important in solvation, and molecular dynamics calculations often show this importance. Recent calculations show that such outer sphere polarizability induced interactions occur in the range of (5 to 10) % of the hydrogen bond strength. This suggests that similar dipole-induced attractive forces occur in these solutions as well.

The dilute volume state for each electrolyte represents solvation (Figure 5a) in the Debye−Hückel limit and is often associated with solvent electrostriction. This ordering of the solvation sphere appears to be systematically disrupted in concentrated solutions. Evidently as concentration increases, for each electrolyte the solvation state has outer sphere water displaced by a counterion (Figure 5b).

Finally, the entropy changes listed for the various volume states show some surprising trends. The four largest are Na_2SO_4, NaF, Na_2CO_3, and NaCl. Among these, NaCl seems to stand out as unusual in this group since it is not clear why its ΔS_i would be so large. Correspondingly, the two smallest ΔS's are NaOH and Na_3PO_4, which seems peculiar since these electrolytes presumably have much more complicated solvation states. As a result, the systematics of ΔS are not yet clear.

SUMMARY

The RLC density model has proven to be very useful for complex Hanford waste liquids despite the limitations noted above. The RLC extensions to molar concentrations appear to provide value for density predictions for volumetric concentrations, which are very useful for process based estimates. The reasons for the significant variability in RLC density predictions are not yet clear, but the RLC model remains very useful in spite of this.

AUTHOR INFORMATION

Corresponding Author

*E-mail: sfagnew@charter.net.

REFERENCES

(1) Laliberte, M.; Cooper, W. E. Model for Calculating the Density of Aqueous Electrolyte Solutions. *J. Chem. Eng. Data* **2004**, *49*, 1141–51.

(2) Reynolds, J. G.; Carter, R. Reconciliation of Solute Concentration Data with Water Contents and Densities of Multi-Component Electrolyte Solutions. *J. Solution Chem.* **2008**, *37*, 1113–25.

(3) Webb, T. J. The Free Energy of Hydration of Ions and the Electrostriction of the Solvent. *J. Am. Chem. Soc.* **1926**, *48*, 2589–2603.

(4) Desnoyers, J. S.; Verrall, R. E.; Conway, B. E. Electrostriction in Aqueous Solutions of Electrolytes. *J. Chem. Phys.* **1965**, *43*, 243.

(5) Marcus, Y. Electrostriction, Ion Solvation, and Solvent Release on Ion Pairing. *J. Phys. Chem. B* **2005**, *109*, 18541–9.

(6) Bobrowski, S. F.; Lee, D. *Tank Waste Information Network System (TWINS)*, PNNL-SA-45730; Pacific Northwest National Laboratory: Richmond, WA, December 2008.

(7) Dittman, G. L. *Calculation of Brine Properties*, UCID-17406; Lawrence Livermore Laboratory: Livermore, CA, February 1977.

(8) Lide, D. R. *CRC Handbook of Physics and Chemistry*, 77th ed.; CRC Press: Boca Raton, FL, 1996; pp 6−139.

(9) Bucher, D.; Kuyucak, S. Polarization of Water in the First hydration Shell of K^+ and Ca^{2+} Ions. *J. Phys. Chem. B* **2008**, *112*, 10786–10790.